HHS Public Access

Author manuscript

Br J Haematol. Author manuscript; available in PMC 2018 April 01.

Published in final edited form as:

Br J Haematol. 2017 April ; 177(2): 271–282. doi:10.1111/bjh.14563.

Anti-leukaemic Activity of the TYK2 selective inhibitor NDI-031301 in T-cell Acute Lymphoblastic Leukaemia

Koshi Akahane[1,2], **Zhaodong Li**[1], **Julia Etchin**[1], **Alla Berezovskaya**[1], **Evisa Gjini**[3], **Craig E. Masse**[4], **Wenyan Miao**[4], **Jennifer Rocnik**[4], **Rosana Kapeller**[4], **Jeremy R. Greenwood**[5], **Hong Tiv**[6], **Takaomi Sanda**[7,8], **David M. Weinstock**[9], and **A. Thomas Look**[1,10,*]

[1] Department of Pediatric Oncology, Dana-Farber Cancer Institute, Harvard Medical School, Boston, MA 02216, USA

[2] Department of Pediatrics, School of Medicine, University of Yamanashi, Chuo, Yamanashi 409-3898, Japan

[3] Center for Immuno - Oncology, Dana-Farber Cancer Institute, Boston, MA 02216, USA

[4] Nimbus Therapeutics, Cambridge, MA 02139, USA

[5] Schrödinger, Inc., New York, NY 10036, USA

[6] Experimental Therapeutics Core, Dana-Farber Cancer Institute, Boston, MA 02210, USA

[7] Cancer Science Institute of Singapore, National University of Singapore, Singapore

[8] Department of Medicine, Yong Loo Lin School of Medicine, National University of Singapore, Singapore

[9] Department of Medical Oncology, Dana-Farber Cancer Institute, Harvard Medical School, Boston, MA 02216, USA

[10] Division of Hematology/Oncology, Boston Children's Hospital, Boston, MA 02115, USA

Summary

Activation of tyrosine kinase 2 (TYK2) contributes to the aberrant survival of T-cell acute lymphoblastic leukaemia (T-ALL) cells. Here we demonstrate the anti-leukaemic activity of a novel TYK2 inhibitor, NDI-031301. NDI-031301 is a potent and selective inhibitor of TYK2 that induced robust growth inhibition of human T-ALL cell lines. NDI-031301 treatment of human T-ALL cell lines resulted in induction of apoptosis that was not observed with the JAK inhibitors tofacitinib and baricitinib. Further investigation revealed that NDI-031301 treatment uniquely

***Corresponding Author:** A. Thomas Look, M.D., Department of Pediatric Oncology, Dana-Farber Cancer Institute, Harvard Medical School, 450 Brookline Ave, Mayer 630, Boston, MA 02216, USA, thomas_look@dfci.harvard.edu, Phone: 617-632-5826, Fax: 617-632-6989.

Author contributions

K.A. designed and performed experiments, analysed data and wrote the manuscript. Z.L. and J.E. helped design and analyse data. A.B. and H.T. performed *in vivo* mouse experiments and analysed data. E.G. helped with the acquisition of data. C.E.M., W.M., J.R. R.K. and J.R.G. designed the NDI-031301 compound and participated in the experimental design. T.S. and D.M.W. designed and analysed research. A.T.L. supervised research, analysed data and co-wrote the manuscript.

Conflict of interest

C.E.M., W.M., J.R. and R.K. are employees of Nimbus Therapeutics and receive compensation and hold equity in the Company. The remaining authors declare no conflict of interest.

leads to activation of three mitogen-activated protein kinases (MAPKs), resulting in phosphorylation of ERK also termed MAPK1), SAPK/JNK (MAPK9/MAPK8) and p38 MAPK (MAPK14) coincident with PARP cleavage. Activation of p38 MAPK occurred within 1 h of NDI-031301 treatment and was responsible for NDI-031301-induced T-ALL cell death, as pharmacological inhibition of p38 partially rescued apoptosis induced by TYK2 inhibitor. Finally, daily oral administration of NDI-031301 at 100 mg/kg bid to immunodeficient mice engrafted with KOPT-K1 T-ALL cells was well tolerated, and led to decreased tumour burden and a significant survival benefit. These results support selective inhibition of TYK2 as a promising potential therapeutic strategy for T-ALL.

Keywords

T-cell acute lymphoblastic leukaemia; TYK2; NDI-031301; p38 MAPK (MAPK14)

Introduction

T-cell acute lymphoblastic leukaemia (T-ALL) is an aggressive haematological malignancy resulting from the transformation of T-cell progenitors and occurs in about 15% of paediatric and 25% of adult ALL cases. The prognosis of this disease has substantially improved due to the introduction of intensified chemotherapy, with cure rates in modern protocols reaching over 75% in children and about 50% in adults (Goldberg, *et al* 2003, Marks, *et al* 2009). Nevertheless, the clinical outcome of T-ALL patients with primary resistant or relapsed disease still remains poor (Goldberg, *et al* 2003, Oudot, *et al* 2008, Schrappe, *et al* 2012), and aggressive treatment regimens are often associated with severe acute toxicities and long-term side effects, including the development of secondary tumours later in life. Thus, development of more effective and less toxic anti-leukaemic drugs have been the focus of research efforts in T-ALL (Aifantis, *et al* 2008).

We have previously demonstrated that tyrosine kinase 2 (TYK2) activation contributes to aberrant survival of human T-ALL cells (Sanda, *et al* 2013). TYK2 is a member of the Janus-activated kinase (JAK) tyrosine kinase family and our report was the first to implicate *TYK2* as an oncogene in T-ALL. Indeed, our gene knockdown experiments showed *TYK2* dependency in 14 of 16 (88%) T-ALL cell lines and 5 of 8 (63%) patient-derived T-ALL cells tested (Sanda, *et al* 2013). In addition, pharmacological inhibition of TYK2 with a small-molecule pan-JAK inhibitor, JAK inhibitor I, induced apoptosis in multiple human T-ALL cell lines (Sanda, *et al* 2013). Our results also showed that *TYK2* promotes the survival of T-ALL cells by upregulating the anti-apoptotic protein BCL2 through phosphorylation and activation of STAT1 (Sanda, *et al* 2013). These findings establish *TYK2* as a promising molecular target for the treatment of T-ALL.

Each of the four JAK family kinases (JAK1, JAK2, JAK3 and TYK2) associates with a distinct set of receptors. Receptor activation triggers receptor intracellular domain phosphorylation, creating docking sites for signal transducers and activators of transcription (STAT) proteins (Ghoreschi, *et al* 2009, Leonard and O'Shea 1998, Liu, *et al* 1998). STAT proteins are subsequently phosphorylated by the JAKs, form homodimers or heterodimers,

translocate to the cell nucleus, and mediate gene transcription. TYK2 is involved in receptor signalling mediated by inflammatory cytokines including the type-I interferons, interleukin (IL)-12 and IL-23 (Ihle, *et al* 1995, Leonard and O'Shea 1998, Liu, *et al* 1998). Therefore TYK2 kinase inhibitors are being developed as potential therapeutics for auto-immune inflammatory diseases, such as psoriasis and inflammatory bowel diseases (Liang, *et al* 2013a, Liang, *et al* 2013b). However, generating kinase inhibitors with a high degree of TYK2 selectivity has posed a significant challenge due to the high sequence homology of the active site among the JAK family kinases. TYK2 specificity is important for clinical application of TYK2 kinase inhibitors, because *Tyk2* knockout mice are viable with normal blood cell counts (Ghoreschi, *et al* 2009, Karaghiosoff, *et al* 2000, Shimoda, *et al* 2000), whereas deficiency of *Jak3* results in severe combined immunodeficiency in mice, and *Jak1* or *Jak2* knockout mice show perinatal lethality (Ghoreschi, *et al* 2009). A loss-of-function mutation in the *TYK2* gene was identified in a patient with hyperimmunoglobulin E syndrome (Minegishi, *et al* 2006), a primary immunodeficiency characterized by elevated serum immunoglobulin E. However, an additional seven individuals with homozygous null mutations of *TYK2* did not have hyperimmunoglobulin E syndrome, but rather exhibited increased susceptibility to mycobacteria or viral infections due to impaired responses to IL-12 and IFN-α/β (Kreins, *et al* 2015). Thus, genetic evidence suggests that pharmacological inhibition of TYK2 should not result in acute toxicity in human patients, but careful monitoring for viral or mycobacterial infections would be warranted in patients treated for prolonged periods.

Here we describe the identification and characterization of the novel highly potent and selective TYK2 inhibitor, NDI-031301. We show that this inhibitor has significant anti-leukaemic activity against human T-ALL cell lines *in vitro* due to its ability to efficiently induce apoptosis in these cells. The inhibitor is orally bioavailable and xenograft studies with a human T-ALL cell line KOPT-K1 showed that it has significant anti-tumour activity *in vivo* without appreciable side effects. Thus, our preclinical findings warrant further testing of NDI-031301 or related compounds as promising drugs for targeted treatment of T-ALL, with the expectation that effective inhibition of the TYK2 pathway would eventually be combined with other anti-leukaemic agents in novel strategies of combination therapy.

Materials and methods

Reagents

NDI-031301 was provided by Nimbus Therapeutics (Cambridge, MA, USA). Tofacitinib baricitinib, trametinib, SP600125, and SB203580 were purchased from Selleck Chemicals (Houston, TX, USA).

Cell culture

All human T-ALL cell lines (KOPT-K1, DU.528, HPB-ALL and SKW-3) were obtained from the American Type Culture Collection (ATCC; Manassas, VA, USA) or Deutsche Sammlung von Mikroorganismen und Zellkulturen GmbH (DSMZ; Braunschweig, Germany). Ba/F3 derivatives expressing various oncogenic fusion kinases, namely, TEL-ABL (ETV6-ABL1), TEL-JAK1 (ETV6-JAK1), TEL-JAK2 (ETV6-JAK2), and TEL-JAK3

(ETV6-JAK3), were obtained from Dr. Richard Morrigl and were described previously (Lacronique, *et al* 2000). Ba/F3 cells transformed by TEL-TYK2 were generated with the pBabe-Neo retroviral vector expressing *ETV6 (TEL)-TYK2* cDNA (Lacronique, *et al* 2000), which was obtained from Dr. Olivier A. Bernard. These cells were maintained in RPMI-1640 medium (GIBCO, Waltham, MA, USA) supplemented with 10% fetal bovine serum (Sigma-Aldrich, St. Louis, MO, USA) and 1% penicillin/streptomycin (Invitrogen, Waltham, MA, USA).

shRNA knockdown experiments

All shRNA constructs cloned into the lentiviral vector pLKO.1-puro were obtained from the RNAi Consortium (Broad Institute, Cambridge, MA, USA). Target sequences for each shRNA are listed in Table SI. Each construct was cotransfected into HEK293T cells with the packaging plasmid psPAX2 and envelope plasmid pMD2.G using FuGENE 6 reagent (Roche, Basel, Switzerland). Supernatants containing the lentivirus were collected and filtered through a 0.45-μm cellulose acetate membrane filter. T-ALL cell lines were then infected with lentivirus in the presence of polybrene (8 μg/ml) and HEPES (10 mM) by centrifugation at 2,500 rpm for 1.5 h at 30°C, and the infected cells were selected by puromycin for at least 36 h.

Cell viability analysis

The Cell Titer Glo assay (Promega, Fitchburg, WI, USA) was used to assess relative cell viability upon treatment. Cells were plated at a density of 5000 - 10000 cells per well in a 96-well plate and incubated with dimethylsulfoxide (DMSO) or increasing concentrations of inhibitor. The relative cell viability was measured after different treatment intervals and reported as a percentage of the DMSO control. The concentration of inhibitor required for 50% inhibition of cell viability (IC_{50}) was determined with GraphPad Prism 6.02 (GraphPad Software, La Jolla, CA, USA).

Apoptosis and cell cycle analysis

Both the terminal deoxynucleotidyl transferase (TdT) dUTP nick-end labeling (TUNEL) assay and propidium iodide (PI) staining were performed with the APO-BrdU™ TUNEL assay kit (Invitrogen, Waltham, MA, USA), according to the manufacturer's recommendation. Briefly, 2×10^6 cells of each treated sample were fixed with 1% paraformaldehyde in phosphate-buffered saline (PBS) for 15 min on ice, washed in PBS and incubated in 70% ethanol at −20°C overnight. After washing and incubation in DNA labeling solution containing TdT and bromodeoxyuridine (BrdU) triphosphates for 4 h at 37°C, the cells were washed and incubated in staining buffer containing an Alexa Fluor 488 dye-labelled anti-BrdU antibody for 30 min of incubation at room temperature, followed by addition of a PI/RNase mixture. After 30 min incubation at room temperature, TUNEL positivity and cell-cycle distribution were analysed with a BD FACSCalibur instrument (BD Biosciences, San Jose, CA, USA). The threshold for TUNEL positivity was determined as the maximal TUNEL signal observed in the untreated cells.

Western blots

Whole-cell lysates were prepared in radioimmunoprecipitation assay (RIPA) buffer (Cell Signaling Tech, Danvers, MA, USA) with FOCUS™ ProteaseArrest™ (G-Biosciences, St. Louis, MO, USA) and Phosphatase Inhibitor Cocktail Set II (EMD Millipore, Billerica, MA, USA). Immunoblotting was performed with specific antibodies to TYK2, STAT1, phospho-STAT1 (Tyr701), STAT3, phospho-STAT3 (Tyr705), STAT5, phospho-STAT5 (Tyr694), STAT6, phospho-STAT6 (Tyr641), AKT, phospho-AKT (Thr308), ERK1/2 (also termed MAPK3/MAPK1), phospho-ERK1/2 (Thr202/Tyr204), SAPK/JNK (also termed MAPK9/MAPK8) (MAPK14), phospho-SAPK/JNK (Thr183/Tyr185), p38 MAPK (also termed MAPK14), phospho-p38 MAPK (Thr180/Tyr182), BCL2, BCL_XL (also termed BCL2L11), MCL1, PARP and α-tubulin (all from Cell Signaling Tech).

T-ALL xenograft model

2×10^6 luciferase-expressing KOPT-K1 cells were injected into the tail vein of 7-week-old female NOD-SCID-IL2Rcγ^{null} (NSG) mice (The Jackson Laboratory, Bar Harbor, ME, USA). The tumour burden was measured by bioluminescence imaging (BLI) every 7 days, using an IVIS Spectrum system (Caliper Life Sciences, Santa Clara, CA, USA). For each BLI time point, cancer bioluminescence was visualized by subcutaneous injection of d-luciferin (Promega) in PBS at 75 mg/kg. After tumour engraftment was established by BLI measurement, mice were divided into 2 groups and treated by oral gavage either with vehicle control (20% HP-β-CD) or NDI-031301 at 100 mg/kg bid (twice daily) for 29 days. After completion of the treatment, 4 mice from each treatment group were sacrificed to obtain femur and spleen. The bone marrow cells were extracted from the femurs by crushing the bone in medium supplemented with 10% fetal bovine serum. The presence of human leukaemia cells was assessed by flow cytometric analysis following staining with fluorescein isothiocynate (FITC)-conjugated anti-human CD45 antibody (Biolegend, San Diego, CA, USA). The femur tissues were also fixed in 10% formalin, sectioned, paraffin-embedded and stained with haematoxylin and eosin. Stained slides were viewed and photographed using an Olympus BX41 microscope and Q-color5 digital camera (Olympus, Center Valley, PA, USA) and imaged with Adobe Photoshop CS4 software (Adobe, San Jose, CA, USA). Survival of the vehicle and NDI-031301 treated mice was defined from initiation of therapy until a moribund state was reached, and was analysed by the Kaplan-Meier method.

Statistical analysis

Statistical significance in assays with identical cell lines was assessed with Student's *t* test (two-tailed). GraphPad Prism 6.02 (GraphPad Software) was used for all statistical analyses. The Calcusyn 2.0 software (Biosoft, Cambridge, UK) was used to analyse combined drug effects and produce the isobolograms normalized to the IC_{50} of each inhibitor.

Results

NDI-031301 is a potent and selective inhibitor of the TYK2 tyrosine kinase

Using a series of proprietary JAK family co-crystal structures in combination with a quantitative computational model to predict selectivity over the JAK family members, we

designed a series of selective TYK2 inhibitors (Wang, *et al* 2015). Elaboration of multiple hit series led to the identification of NDI-031301 as an inhibitor that is preferentially active against TYK2 compared to other JAK family kinases. Preclinical studies have illustrated that NDI-031301 potently inhibits targeted immune cell cytokine signalling and demonstrates outstanding efficacy in ameliorating disease in mouse models of psoriasis (Miao, *et al* 2015). The profile of NDI-031301, including the results of the biochemical TYK2 kinase assay, biochemical JAK family selectivity, plasma protein binding, and pharmacokinetic parameters in mice after oral administration are shown in Table I.

To assess the cellular activity and selectivity of NDI-031301 for TYK2, we tested its ability of this drug to inhibit the proliferation of Ba/F3 cells transformed by each of a series of constitutively active JAK family kinases (TEL-JAK1, TEL-JAK2, TEL-JAK3 and TEL-TYK2) or by a more distantly related tyrosine kinase, TEL-ABL (Fig 1A). NDI-031301 most strongly inhibited the growth of TYK2-transfomed cells, with the IC_{50} of 1.583 μM following 72 h of exposure, whereas Ba/F3 cells transformed by other tyrosine kinases showed decreased sensitivity to this drug (Fig 1D). Tofacitinib (JAK1, JAK2 and JAK3 inhibitor) and baricitinib (JAK1 and JAK2 inhibitor) were less effective inhibitors than NDI-031301 on the proliferation of TYK2-transformed cells, with IC_{50} values of 23.89 μM (tofacitinib) and 3.98 μM (baricitinib) after 72 h of treatment, while these drugs were highly active against Ba/F3 cells transformed by the other JAK family kinases (Fig 1B, C and D). These results demonstrate that NDI-031301 is a selective inhibitor of TYK2 tyrosine kinase with activity in cells transduced and rendered IL-3-independent by an activated form of this kinase.

NDI-031301 induces growth inhibition and apoptosis in human T-ALL cell lines

To assess the anti-tumour potency of NDI-031301 against T-ALL, we tested the inhibitory effect of this drug on the proliferation of multiple T-ALL cell lines (Fig 2A). This agent induced remarkable cytotoxicity in each of 4 human T-ALL cell lines representing different molecular subtypes of the disease (DU.528, KOPT-K1, HPB-ALL and SKW-3), with IC_{50} values of 0.8186 – 2.38 μM after 72 h of exposure (Fig 2D). This inhibitory effect was more potent than that of either tofacitinib or baricitinib, except that DU.528 cells were highly sensitive to all JAK kinase inhibitors tested in this study (Fig 2B, C and D). To gain insight into the cytotoxic mechanism triggered by NDI-031301, we next monitored changes in the relative numbers of KOPT-K1 cells treated with NDI-031301 over a 5-day period. As shown in Figure 2E, DMSO-treated KOPT-K1 cells demonstrated exponential growth while NDI-031301 treatment demonstrated dose-dependent growth suppression, with 1 μM NDI-031301 causing minor growth suppression of KOPTK1 cells and 3 μM NDI-031301 treatment reducing total cell number 8-fold on the fifth day of treatment, as compared to cell numbers at Day 0. Moreover, we demonstrated that NDI-031301 caused a profound apoptotic response in the KOPT-K1 cells, as shown by the appearance of 31.1% apoptotic cells following treatment with 3μM NDI-031301 for 48 h in a TUNEL apoptotic assay (Fig 2F). An increased level of apoptosis in KOPT-K1 cells was also observed at 24 h after treatment with 3 μM NDI-031301 by flow cytometric analysis following Annexin V-FITC and PI double staining (Fig S1).

TYK2 inhibition leads not only to suppression of STAT1 phosphorylation, but also activation of MAPK signalling pathways in KOPT-K1 cells

Our previous results indicated that TYK2 acts to upregulate levels of the anti-apoptotic protein BCL2 in T-ALL cells through phosphorylation and activation of STAT1 (Sanda, *et al* 2013). However, this is not the only pathway involved in TYK2-mediated promotion of survival, because a specific inhibitor of BCL2, ABT-199, is not active in the killing of most T-ALL cells (Anderson, *et al* 2014, Chonghaile, *et al* 2014, Peirs, *et al* 2014). Rather, only T-ALL cells with an early T-cell progenitor (ETP) phenotype show enhanced sensitivity to ABT-199 (Anderson, *et al* 2014, Chonghaile, *et al* 2014, Peirs, *et al* 2014), implying that other mechanisms in addition to the downregulation of the STAT1-BCL2 signalling contribute to the induction of apoptosis by TYK2 inhibition. Thus, we investigated cellular signalling pathways that are associated with cell survival and specifically affected by TYK2 inhibition with NDI-031301. We treated KOPT-K1 cells with NDI-031301, tofacitinib, or baricitinib for 24 h, and then examined the levels of total and phosphorylated protein of known cell survival signalling pathways (Fig 3A). Two drug concentrations, 1 μM and 3 μM, of NDI-031301 were selected for this assay because this compound had produced a dose-dependent inhibitory effect on TYK2-transformed Ba/F3 cells (Fig 1A) as well as KOPT-K1 cells (Fig 2A) over this concentration range. The concentrations of tofacitinib (1 μM) and baricitinib (300 nM) were determined from the results of the Ba/F3 assay, in which these concentrations efficiently inhibited the proliferation of Ba/F3 cells transformed by corresponding JAK kinases, without affecting the viability of TYK2-transformed cells (Fig 1B and C).

The results in Figure 3A indicate that treatment with 3 μM of NDI-031301 leads to reduction of STAT1 Tyr-701 phosphorylation and BCL2 protein levels in KOPT-K1 cells, consistent with our previous finding that TYK2 phosphorylates STAT1 and upregulates BCL2 expression in most T-ALL cells (Sanda, *et al* 2013). Decreased levels of STAT1 Tyr-701 phosphorylation were also observed in cells treated with tofacitinib or baricitinib, demonstrating that this activity is not specific to TYK2 inhibition and that other JAK kinases are involved in the regulation of STAT1 Tyr-701 phosphorylation in KOPT-K1 cells. The phosphorylation levels of STAT3 (Tyr-705), STAT5 (Tyr-694) and STAT6 (Tyr-641) were not affected by treatment with either NDI-031301 or other JAK kinase inhibitors (Fig 3A). The levels of AKT Thr-308 phosphorylation were also unchanged after each of the treatments (Fig 3A). We found that each of the mitogen-activated protein kinase (MAPK) pathways were activated specifically by treatment with 3 μM of NDI-031301, as indicated by increased phosphorylation levels of ERK1/2 (Thr-202/Tyr-204), SAPK/JNK (Thr-183/Tyr-185), and p38 MAPK (Thr-180/Tyr-182) (Fig 3A). Importantly, efficient induction of apoptosis was observed only in the cells treated with 3 μM of NDI-031301, as indicated by the presence of cleaved PARP (Fig 3A). These results indicate that downregulation of STAT1 Tyr-701 phosphorylation is not sufficient by itself to induce apoptosis in KOPT-K1 cells, suggesting instead that activation of the MAPK pathways might also play a role in NDI-031301-induced apoptosis in these cells.

We then asked whether the effect of NDI-031301 on cellular signalling could be recapitulated by gene knockdown of *TYK2*. Silencing of *TYK2* by lentiviral shRNA

knockdown (shTYK2 2 and 3) resulted in elimination of STAT1 Tyr-701 phosphorylation in KOPT-K1 cells (Fig 3B), consistent with the result in the cells treated with NDI-031301 (Fig 3A). The increased phosphorylation levels of SAPK/JNK (Thr-183/Tyr-185) and p38 MAPK (Thr-180/Tyr-182) were clearly observed in the cells transfected with *TYK2*-targeting shRNAs, while the levels of ERK1/2 phosphorylation (Thr-202/Tyr-204) were not upregulated (Fig 3B). Thus, TYK2 signalling is required for the down-modulation of the SAPK/JNK and p38 MAPK pathways in KOPT-K1 cells, as indicated both genetically and by NDI-031301-mediated inhibition of TYK2 tyrosine kinase activity.

Activation of p38 MAPK is involved in NDI-031301-induced apoptosis in KOPT-K1 cells

Previous studies have shown that the SAPK/JNK and p38 MAPK pathways play key roles in the negative selection of $CD4^+/CD8^+$ thymocytes (Rincon and Davis 2009, Sohn, *et al* 2003, Sohn, *et al* 2007, Sugawara, *et al* 1998, Tanaka, *et al* 2002), an essential process by which self-reactive T-cells are removed from the host. Thus, we hypothesized that activated MAPK pathways are also involved in NDI-031301-mediated apoptosis in T-ALL cells. Time-course analyses with KOPT-K1 cells demonstrated that a dramatic increase in levels of p38 MAPK phosphorylation (Thr-180/Tyr-182) and a decrease in levels of STAT1 phosphorylation (Tyr-701) occurred at 1 h after treatment with 3 μM of NDI-031301, while increased levels of ERK1/2 Thr-202/Tyr-204 and SAPK/JNK Thr-183/Tyr-185 phosphorylation were observed after 8 h of treatment (Fig 4A). Cleaved PARP was first detected at 12 h of treatment (Fig 4A). These results indicate that NDI-031301 mediates activation of the MAPK pathways before the induction of apoptosis.

We next determined whether pharmacological inhibition of each MAPK pathway could protect T-ALL cells from proliferative suppression and apoptosis induced by NDI-031301. We treated KOPT-K1 cells for 72 h with 0 to 3 μM of NDI-031301 in combination with each of the following MAPK pathway inhibitors: SB203580 (p38 MAPK inhibitor; 0, 5 and 10 μM), trametinib (MEK1/2 inhibitor; 0, 1.25 and 2.5 nM) and SP600125 (SAPK/JNK inhibitor; 0 and 5 μM), and then assessed the cell proliferative responses. We found that combined treatment with SB203580 partially rescued the NDI-031301-induced decrease of viability in KOPT-K1 cells (Fig 4B). Isobologram analysis indicated that this combination produced remarkable antagonism between the two inhibitors in decreasing cell viability, as indicated by the average combination index (CI) value of 2.06 (Fig 4C). Combination with trametinib or SP600125 showed no rescue effects on the viability of KOPT-K1 cells treated with NDI-031301 (Fig S2A and C) with only modest antagonism for combination with trametinib (average CIs: 1.39) (Fig S2B) or SP600125 (average CIs: 1.15) (Fig S2D). SB203580 also partially rescued NDI-031301-induced apoptosis in KOPT-K1 cells, as indicated by a decrease in TUNEL positivity (Fig 4D), and an absence or decreased levels of cleaved PARP induced by 3 μM of NDI-031301 (Fig 4E). We also found that SB203580 efficiently inhibited NDI-031301-mediated increase of levels of p38 MAPK Thr-180/Tyr-182 phosphorylation without downregulating the levels of ERK1/2 Thr-202/Tyr-204 and SAPK/JNK Thr-183/Tyr-185 phosphorylation (Fig 4E). These results demonstrate that activation of the p38 MAPK pathway, but not the ERK or SAPK/JNK pathways, is at least partially responsible for NDI-031301-induced apoptosis in KOPT-K1 cells, indicating involvement of the p38 MAPK pathway in TYK2-mediated survival in T-ALL cells. Further

investigation to assess NDI-031301 sensitivity and the effect of the drug treatment on cellular signalling pathways in an additional 3 T-ALL cell lines indicated variable levels of increased phosphorylation of p38 MAPK and downregulation of BCL2 that did not clearly correlate with the IC_{50} values for NDI-031301 in these cell lines (Fig S3A-D). Thus, there appears to be considerable heterogeneity in altered signal transduction in the different cell lines after treatment with NDI-031301 in the timing and magnitude of the response, which is expected given the wide heterogeneity of oncogenic mutations and chromosomal abnormalities among these T-ALL cell lines.

NDI-031301 suppresses the proliferation of T-ALL cells in vivo

We then tested the efficacy of NDI-031301 *in vivo* using a murine xenograft model. By injecting NSG mice with 2×10^6 KOPT-K1 cells expressing luciferase, we were able to quantify leukaemia growth by BLI. Once tumour engraftment was established by BLI (Fig 5A), treatment with either vehicle or 100 mg/kg NDI-031301 twice daily was initiated and continued for 29 days. This dosage of NDI-031301 was well tolerated by the mice without any appreciable side effects and body weight loss (Fig S4). We found that treatment with NDI-031301 significantly delayed tumour progression in this model (Fig 5B and C): mean bioluminescence on day 42 was 3.126×10^{10}/photons (ph)/s/cm^2/steradian (sr) for vehicle control, versus 1.277×10^{10}/ph/s/cm^2/sr for NDI-031301-treated animals ($P < 0.0001$; n = 6 in each group). As a result, NDI-031301 significantly increased overall survival compared with vehicle treatment ($P = 0.0064$; n = 6 in each group) (Fig 5D).

After 29 days of treatment, mice receiving NDI-031301 had marked reductions in splenomegaly by comparison with controls (Fig 6A and B). Flow cytometric analysis to detect human CD45-positive cells showed a significant decrease in the extent of leukaemic cell infiltration in the femur bone marrow of NDI-031301-treated mice versus vehicle-treated mice (Fig 6C and D). Decreased numbers of human leukaemia cells after NDI-031301 treatment were also observed in the peripheral blood (Fig S5). Histopathological analysis of the bone marrow of the vehicle-treated mice showed massive infiltration by leukaemic cells (Fig 6E), while NDI-031301 treatment suppressed leukaemic cell infiltration (Fig 6F). Taken together, our results demonstrate that NDI-031301 is efficacious in delaying the growth of human T-ALL cells *in vivo* and in extending the survival of mice bearing human T-ALL cells.

Discussion

Here we report that TYK2 inhibition by a small-molecule inhibitor, NDI-031301, results in robust anti-tumour activity in T-ALL cells. We found that NDI-031301 shows selective inhibitory activity against TYK2 as compared to other JAK kinases in living cells, as indicated by transformed Ba/F3 assays. This inhibitor induced cytotoxicity in 4 representative human T-ALL cell lines, consistent with our previous result showing the growth and survival inhibition of these cells by silencing *TYK2* with shRNA (Sanda, *et al* 2013). Finally, the anti-leukaemic activity of NDI-031301 was recapitulated in a KOPT-K1 *in vivo* xenograft study, indicating that this inhibitor is able to efficiently suppress the growth of human T-ALL cells *in vivo* as well as *in vitro*.

Our results also indicated that in the KOPT-K1 T-ALL cell line, activation of three different MAPK signalling pathways was observed after treatment with NDI-031301. However, of these pathways, only the activation of p38 MAPK contributed to apoptosis induced by this inhibitor. Increased phosphorylation levels of p38 MAPK (Thr-180/Tyr-182) were also observed in the cells transfected with each of two different shRNAs targeting *TYK2* (Fig 3B), indicating that NDI-031301-mediated activation of p38 MAPK is probably mediated through inhibition of TYK2. Time-course analyses with KOPT-K1 cells demonstrated elevated levels of p38 MAPK phosphorylation (Thr-180/Tyr-182), as observed at 1 h post-treatment with NDI-031301, suggesting that TYK2 negatively regulates proteins that control the activation of p38 MAPK in T-ALL cells. Previous studies have shown a critical role for p38 MAPK pathway activation in the anti-leukaemic effects of dasatinib (Dumka, *et al* 2009), imatinib (Parmar, *et al* 2004) and IFNα (Mayer, *et al* 2001) in BCR-ABL-transformed cells; however, our finding is the first to demonstrate involvement of p38 MAPK pathway activation in T-ALL cell death occurring after TYK2 inhibition. We did not find clear association between variable levels of phosphorylation of p38 MAPK and differential NDI-031301 sensitivities in human T-ALL cell lines (Fig 4A and Fig S3A-D), suggesting that the consequences of p38 MAPK activation are highly context-dependent and probably differ based on the wide genetic and phenotypic heterogeneity among individual T-ALL cases. Importantly, activation of p38 MAPK is associated with the deletion of $CD4^+CD8^+$ double-positive thymocytes by negative selection (Rincon and Davis 2009, Sohn, *et al* 2003, Sohn, *et al* 2007, Sugawara, *et al* 1998, Tanaka, *et al* 2002), although the mechanism of this effect still remains to be established. It is conceivable that TYK2 normally promotes the survival of a subset of developing thymocytes, and that this pathway becomes essential for the survival of transformed T-ALL cells.

Our findings clearly support TYK2 inhibition with NDI-031301 or a related compound as a potential therapeutic strategy for patients with T-ALL, and also raise the possibility that enhancing p38 MAPK activation in T-ALL cells may be an approach to accentuate its anti-leukaemic activity. Further preclinical studies with selective TYK2 inhibitors, both alone and in combination with other targeted inhibitors, are needed to delineate an optimal strategy for targeting this pathway, which will be essential for the design of early stage clinical trials to incorporate TYK2 inhibition into available regimens for the treatment of patients with T-ALL.

Supplementary Material

Refer to Web version on PubMed Central for supplementary material.

Acknowledgements

This work was supported by fellowships and grants from the Leukemia & Lymphoma Society (CDP5014-14; K.A.) and William Lawrence Blanche Hughes foundation (A.T.L.), a bridge grant from Alex's Lemonade Stand Foundation (A.T.L.), and grants 5R01CA176746 (A.T.L.) and 1R35 CA210064-01 (A.T.L.) from the National Cancer Institute. Z.L. is funded by Alex's Lemonade Stand Foundation. J.E. is supported by Alex's Lemonade Stand Foundation, The Wong Family Award, Claudia Adams Barr Program for Innovative Cancer Research and Luck2Tuck Foundation. T.S. is supported by a grant from the National Research Foundation, Prime Minister's Office, Singapore under its NRF Fellowship Programme (Award No. NRF-NRFF2013-02). D.M.W. is supported by grants 2R01CA15189806A1 and 4R01CA17238704 from the National Cancer Institute. Funds for *in vivo*

experiments in NSG mice were provided by Nimbus Therapeutics. We thank John R. Gilbert for critical review of the manuscript and editorial suggestions. We also thank Nimbus Therapeutics for the compound NDI-031301.

References

Aifantis I, Raetz E, Buonamici S. Molecular pathogenesis of T-cell leukaemia and lymphoma. Nat Rev Immunol. 2008; 8:380–390. [PubMed: 18421304]

Anderson NM, Harrold I, Mansour MR, Sanda T, McKeown M, Nagykary N, Bradner JE, Lan Zhang G, Look AT, Feng H. BCL2-specific inhibitor ABT-199 synergizes strongly with cytarabine against the early immature LOUCY cell line but not more-differentiated T-ALL cell lines. Leukemia. 2014; 28:1145–1148. [PubMed: 24342948]

Chonghaile TN, Roderick JE, Glenfield C, Ryan J, Sallan SE, Silverman LB, Loh ML, Hunger SP, Wood B, DeAngelo DJ, Stone R, Harris M, Gutierrez A, Kelliher MA, Letai A. Maturation stage of T-cell acute lymphoblastic leukemia determines BCL-2 versus BCL-XL dependence and sensitivity to ABT-199. Cancer Discov. 2014; 4:1074–1087. [PubMed: 24994123]

Dumka D, Puri P, Carayol N, Lumby C, Balachandran H, Schuster K, Verma AK, Terada LS, Platanias LC, Parmar S. Activation of the p38 Map kinase pathway is essential for the antileukemic effects of dasatinib. Leuk Lymphoma. 2009; 50:2017–2029. [PubMed: 19672773]

Ghoreschi K, Laurence A, O'Shea JJ. Janus kinases in immune cell signaling. Immunol Rev. 2009; 228:273–287. [PubMed: 19290934]

Goldberg JM, Silverman LB, Levy DE, Dalton VK, Gelber RD, Lehmann L, Cohen HJ, Sallan SE, Asselin BL. Childhood T-cell acute lymphoblastic leukemia: the Dana-Farber Cancer Institute acute lymphoblastic leukemia consortium experience. J Clin Oncol. 2003; 21:3616–3622. [PubMed: 14512392]

Ihle JN, Witthuhn BA, Quelle FW, Yamamoto K, Silvennoinen O. Signaling through the hematopoietic cytokine receptors. Annu Rev Immunol. 1995; 13:369–398. [PubMed: 7612228]

Karaghiosoff M, Neubauer H, Lassnig C, Kovarik P, Schindler H, Pircher H, McCoy B, Bogdan C, Decker T, Brem G, Pfeffer K, Muller M. Partial impairment of cytokine responses in Tyk2-deficient mice. Immunity. 2000; 13:549–560. [PubMed: 11070173]

Kreins AY, Ciancanelli MJ, Okada S, Kong XF, Ramirez-Alejo N, Kilic SS, El Baghdadi J, Nonoyama S, Mahdaviani SA, Ailal F, Bousfiha A, Mansouri D, Nievas E, Ma CS, Rao G, Bernasconi A, Sun Kuehn H, Niemela J, Stoddard J, Deveau P, Cobat A, El Azbaoui S, Sabri A, Lim CK, Sundin M, Avery DT, Halwani R, Grant AV, Boisson B, Bogunovic D, Itan Y, Moncada-Velez M, Martinez-Barricarte R, Migaud M, Deswarte C, Alsina L, Kotlarz D, Klein C, Muller-Fleckenstein I, Fleckenstein B, Cormier-Daire V, Rose-John S, Picard C, Hammarstrom L, Puel A, Al-Muhsen S, Abel L, Chaussabel D, Rosenzweig SD, Minegishi Y, Tangye SG, Bustamante J, Casanova JL, Boisson-Dupuis S. Human TYK2 deficiency: Mycobacterial and viral infections without hyper-IgE syndrome. J Exp Med. 2015; 212:1641–1662. [PubMed: 26304966]

Lacronique V, Boureux A, Monni R, Dumon S, Mauchauffe M, Mayeux P, Gouilleux F, Berger R, Gisselbrecht S, Ghysdael J, Bernard OA. Transforming properties of chimeric TEL-JAK proteins in Ba/F3 cells. Blood. 2000; 95:2076–2083. [PubMed: 10706877]

Leonard WJ, O'Shea JJ. Jaks and STATs: biological implications. Annu Rev Immunol. 1998; 16:293–322. [PubMed: 9597132]

Liang J, Tsui V, Van Abbema A, Bao L, Barrett K, Beresini M, Berezhkovskiy L, Blair WS, Chang C, Driscoll J, Eigenbrot C, Ghilardi N, Gibbons P, Halladay J, Johnson A, Kohli PB, Lai Y, Liimatta M, Mantik P, Menghrajani K, Murray J, Sambrone A, Xiao Y, Shia S, Shin Y, Smith J, Sohn S, Stanley M, Ultsch M, Zhang B, Wu LC, Magnuson S. Lead identification of novel and selective TYK2 inhibitors. Eur J Med Chem. 2013a; 67:175–187. [PubMed: 23867602]

Liang J, van Abbema A, Balazs M, Barrett K, Berezhkovsky L, Blair W, Chang C, Delarosa D, DeVoss J, Driscoll J, Eigenbrot C, Ghilardi N, Gibbons P, Halladay J, Johnson A, Kohli PB, Lai Y, Liu Y, Lyssikatos J, Mantik P, Menghrajani K, Murray J, Peng I, Sambrone A, Shia S, Shin Y, Smith J, Sohn S, Tsui V, Ultsch M, Wu LC, Xiao Y, Yang W, Young J, Zhang B, Zhu BY, Magnuson S. Lead optimization of a 4-aminopyridine benzamide scaffold to identify potent, selective, and orally bioavailable TYK2 inhibitors. J Med Chem. 2013b; 56:4521–4536. [PubMed: 23668484]

Liu KD, Gaffen SL, Goldsmith MA. JAK/STAT signaling by cytokine receptors. Curr Opin Immunol. 1998; 10:271–278. [PubMed: 9638363]

Marks DI, Paietta EM, Moorman AV, Richards SM, Buck G, DeWald G, Ferrando A, Fielding AK, Goldstone AH, Ketterling RP, Litzow MR, Luger SM, McMillan AK, Mansour MR, Rowe JM, Tallman MS, Lazarus HM. T-cell acute lymphoblastic leukemia in adults: clinical features, immunophenotype, cytogenetics, and outcome from the large randomized prospective trial (UKALL XII/ECOG 2993). Blood. 2009; 114:5136–5145. [PubMed: 19828704]

Mayer IA, Verma A, Grumbach IM, Uddin S, Lekmine F, Ravandi F, Majchrzak B, Fujita S, Fish EN, Platanias LC. The p38 MAPK pathway mediates the growth inhibitory effects of interferon-alpha in BCR-ABL-expressing cells. J Biol Chem. 2001; 276:28570–28577. [PubMed: 11353767]

Miao WY, Masse C, Greenwood J, Kapeller R, Westlin W. Potent and Selective Tyk2 Inhibitors Block Th1-and Th17-Mediated Immune Responses and Reduce Disease Progression in Rodent Models of Delayed-Type Hypersensitivity and Psoriasis. Arthritis Rheumatol. 2015; 67(Supplement 10) Meeting Abstract: 1943.

Minegishi Y, Saito M, Morio T, Watanabe K, Agematsu K, Tsuchiya S, Takada H, Hara T, Kawamura N, Ariga T, Kaneko H, Kondo N, Tsuge I, Yachie A, Sakiyama Y, Iwata T, Bessho F, Ohishi T, Joh K, Imai K, Kogawa K, Shinohara M, Fujieda M, Wakiguchi H, Pasic S, Abinun M, Ochs HD, Renner ED, Jansson A, Belohradsky BH, Metin A, Shimizu N, Mizutani S, Miyawaki T, Nonoyama S, Karasuyama H. Human tyrosine kinase 2 deficiency reveals its requisite roles in multiple cytokine signals involved in innate and acquired immunity. Immunity. 2006; 25:745–755. [PubMed: 17088085]

Oudot C, Auclerc MF, Levy V, Porcher R, Piguet C, Perel Y, Gandemer V, Debre M, Vermylen C, Pautard B, Berger C, Schmitt C, Leblanc T, Cayuela JM, Socie G, Michel G, Leverger G, Baruchel A. Prognostic factors for leukemic induction failure in children with acute lymphoblastic leukemia and outcome after salvage therapy: the FRALLE 93 study. J Clin Oncol. 2008; 26:1496–1503. [PubMed: 18349402]

Parmar S, Katsoulidis E, Verma A, Li Y, Sassano A, Lal L, Majchrzak B, Ravandi F, Tallman MS, Fish EN, Platanias LC. Role of the p38 mitogen-activated protein kinase pathway in the generation of the effects of imatinib mesylate (STI571) in BCR-ABL-expressing cells. J Biol Chem. 2004; 279:25345–25352. [PubMed: 15056660]

Peirs S, Matthijssens F, Goossens S, Van de Walle I, Ruggero K, de Bock CE, Degryse S, Cante-Barrett K, Briot D, Clappier E, Lammens T, De Moerloose B, Benoit Y, Poppe B, Meijerink JP, Cools J, Soulier J, Rabbitts TH, Taghon T, Speleman F, Van Vlierberghe P. ABT-199 mediated inhibition of BCL-2 as a novel therapeutic strategy in T-cell acute lymphoblastic leukemia. Blood. 2014; 124:3738–3747. [PubMed: 25301704]

Rincon M, Davis RJ. Regulation of the immune response by stress-activated protein kinases. Immunol Rev. 2009; 228:212–224. [PubMed: 19290930]

Sanda T, Tyner JW, Gutierrez A, Ngo VN, Glover J, Chang BH, Yost A, Ma W, Fleischman AG, Zhou W, Yang Y, Kleppe M, Ahn Y, Tatarek J, Kelliher M, Neuberg D, Levine RL, Moriggl R, Muller M, Gray NS, Jamieson CH, Weng AP, Staudt LM, Druker BJ, Look AT. TYK2-STAT1-BCL2 Pathway Dependence in T-Cell Acute Lymphoblastic Leukemia. Cancer Discov. 2013; 3:564–577. [PubMed: 23471820]

Schrappe M, Hunger SP, Pui CH, Saha V, Gaynon PS, Baruchel A, Conter V, Otten J, Ohara A, Versluys AB, Escherich G, Heyman M, Silverman LB, Horibe K, Mann G, Camitta BM, Harbott J, Riehm H, Richards S, Devidas M, Zimmermann M. Outcomes after induction failure in childhood acute lymphoblastic leukemia. N Engl J Med. 2012; 366:1371–1381. [PubMed: 22494120]

Shimoda K, Kato K, Aoki K, Matsuda T, Miyamoto A, Shibamori M, Yamashita M, Numata A, Takase K, Kobayashi S, Shibata S, Asano Y, Gondo H, Sekiguchi K, Nakayama K, Nakayama T, Okamura T, Okamura S, Niho Y, Nakayama K. Tyk2 plays a restricted role in IFN alpha signaling, although it is required for IL-12-mediated T cell function. Immunity. 2000; 13:561–571. [PubMed: 11070174]

Sohn SJ, Rajpal A, Winoto A. Apoptosis during lymphoid development. Curr Opin Immunol. 2003; 15:209–216. [PubMed: 12633672]

Sohn SJ, Thompson J, Winoto A. Apoptosis during negative selection of autoreactive thymocytes. Curr Opin Immunol. 2007; 19:510–515. [PubMed: 17656079]

Sugawara T, Moriguchi T, Nishida E, Takahama Y. Differential roles of ERK and p38 MAP kinase pathways in positive and negative selection of T lymphocytes. Immunity. 1998; 9:565–574. [PubMed: 9806642]

Tanaka N, Kamanaka M, Enslen H, Dong C, Wysk M, Davis RJ, Flavell RA. Differential involvement of p38 mitogen-activated protein kinase kinases MKK3 and MKK6 in T-cell apoptosis. EMBO Rep. 2002; 3:785–791. [PubMed: 12151339]

Wang L, Wu Y, Deng Y, Kim B, Pierce L, Krilov G, Lupyan D, Robinson S, Dahlgren MK, Greenwood J, Romero DL, Masse C, Knight JL, Steinbrecher T, Beuming T, Damm W, Harder E, Sherman W, Brewer M, Wester R, Murcko M, Frye L, Farid R, Lin T, Mobley DL, Jorgensen WL, Berne BJ, Friesner RA, Abel R. Accurate and reliable prediction of relative ligand binding potency in prospective drug discovery by way of a modern free-energy calculation protocol and force field. J Am Chem Soc. 2015; 137:2695–2703. [PubMed: 25625324]

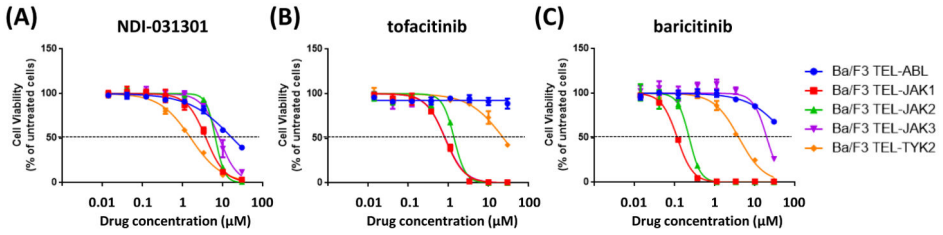

(D)

Assay IC_{50}	NDI-031301 (μM)	tofacitinib (μM)	baricitinib (μM)
Ba/F3 TEL-ABL	17.4	No response	67.36
Ba/F3 TEL-JAK1	3.809	0.8223	0.1157
Ba/F3 TEL-JAK2	6.571	1.386	0.23
Ba/F3 TEL-JAK3	8.21	0.8372	19.87
Ba/F3 TEL-TYK2	1.583	23.89	3.98

Fig 1. NDI-031301 is a potent and selective inhibitor of TYK2 tyrosine kinase

(A-C) Anti-proliferative activity of NDI-031301 (A), tofacitinib (B) or baricitinib (C) on transformed Ba/F3 cells. Ba/F3 cells transformed by TEL-ABL, TEL-JAK1, TEL-JAK2, TEL-JAK3, or TEL-TYK2 were cultured with graded concentrations of the indicated inhibitor for 72 h. Cell viability values are mean ± s.d. percentages of the untreated control value in triplicate experiments. **(D)** 50% inhibitory concentration (IC_{50}) values for NDI-031301, tofacitinib and baricitinib in Fig 1A-C.

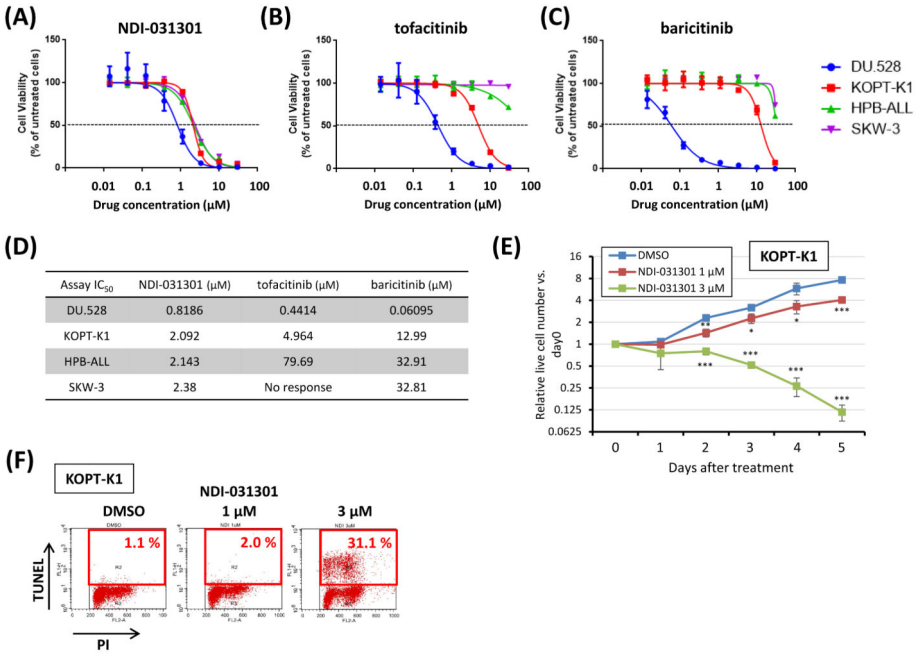

Assay IC_{50}	NDI-031301 (μM)	tofacitinib (μM)	baricitinib (μM)
DU.528	0.8186	0.4414	0.06095
KOPT-K1	2.092	4.964	12.99
HPB-ALL	2.143	79.69	32.91
SKW-3	2.38	No response	32.81

Fig 2. NDI-031301 induces growth inhibition and apoptosis in human T-ALL cell lines

(A-C) Anti-proliferative activity of NDI-031301 (A), tofacitinib (B), or baricitinib (C) on human T-ALL cell lines. DU.528, KOPT-K1, HPB-ALL and SKW-3 cells were cultured with graded concentrations of the indicated inhibitor for 72 h. Cell viability values are mean ± s.d. percentages of the untreated control value in triplicate experiments. **(D)** 50% inhibitory concentration (IC_{50}) values for NDI-031301, tofacitinib and baricitinib in Fig 2A-C. **(E)** KOPT-K1 cells were cultured in 0, 1 μM, or 3 μM of NDI-031301, and the number of viable cells was measured with trypan blue staining. Values are mean ± s.d. fold changes relative to Day 0 in triplicate experiments. * $P < 0.05$; ** $P < 0.01$; *** $P < 0.001$ by two-sample, two-tailed *t* test. **(F)** KOPT-K1 cells were cultured in 0, 1 μM, or 3 μM of NDI-031301 for 48 h. Cells were fixed, and assessed for apoptosis and cell-cycle distribution by flow cytometric analysis after terminal deoxynucleotidyl transferase (TdT) dUTP nick-end labeling (TUNEL) and proppidium iodide (PI) double labelling. The panels show two-dimensional dot plots with the percentage of TUNEL-positive cells in each sample.

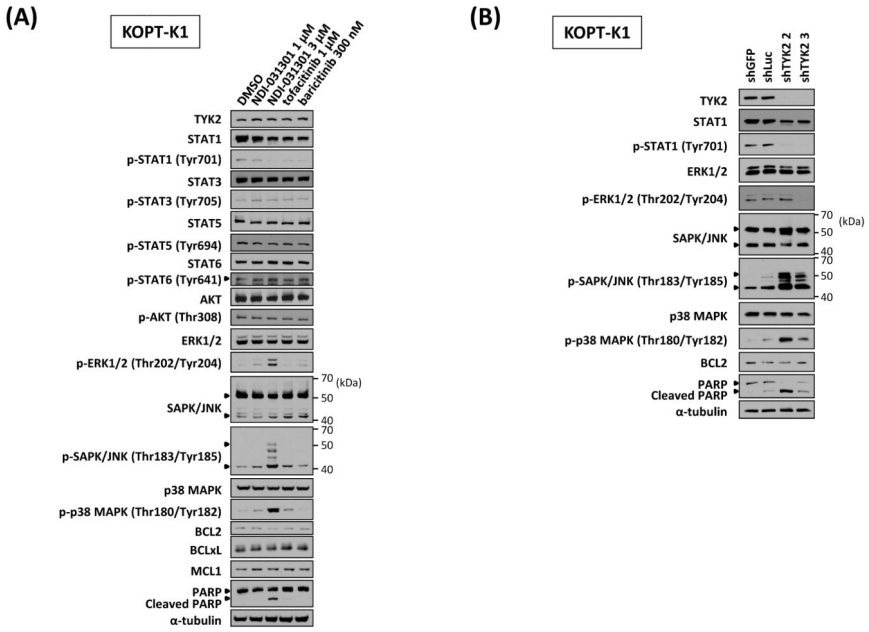

Fig 3. TYK2 inhibition leads to activation of the MAPK signalling pathways as well as downregulation of phospho-STAT1 in KOPT-K1 cells

(A) Western blot analysis to assess the effect of each JAK kinase inhibitor on cellular signalling pathways in KOPT-K1 cells. KOPT-K1 cells were treated with the indicated concentrations of NDI-031301, tofacitinib or baricitinib for 24 h, and subjected to immunoblot analysis with each specified antibody. **(B)** KOPT-K1 cells were lentivirally transduced with *TYK2*-targeting shRNAs (shTYK2 2 and 3) or control shRNAs targeting GFP (shGFP) or luciferase (shLuc). Whole-cell extracts were analyzed by immunoblotting with each specified antibody.

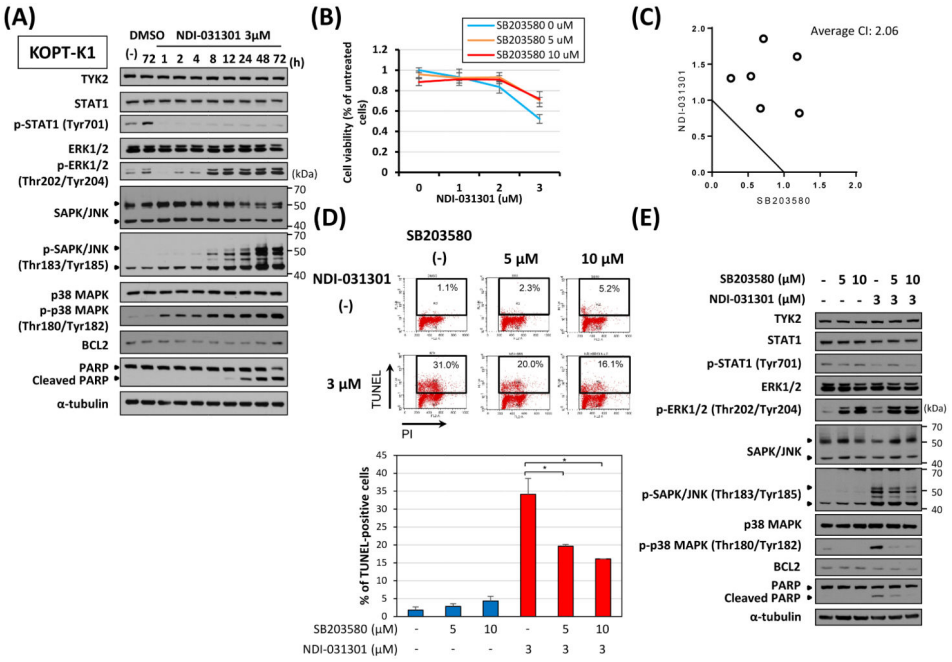

Fig 4. Activation of p38 MAPK is involved in NDI-031301-induced apoptosis in KOPT-K1 cells

(A) Time-course analysis to assess the effect of NDI-031301 on cellular signalling pathways in KOPT-K1 cells. The cells were treated with dimethyl sulfoxide (DMSO) or 3 μM of NDI-031301, and harvested at the indicated times. Western blot analysis was conducted with each specified antibody. **(B-C)** KOPT-K1 cells were treated for 72 h with serial dilutions of NDI-031301 (0 - 3 μM) and p38 MAPK pathway inhibitor SB203580 (0 - 10 μM) in combination. Relative cell viability is shown in panel (B), as mean ± s.d. percentages of the DMSO-treated control value in triplicate experiment. The normalized isobologram was obtained with the Calcusyn software. The combination index (CI) was plotted as a function of dose combination and an average CI of the drug combination is indicated in panel (C). The additive isobole is depicted as a straight line, with antagonistic dose combinations labelled above the isobole. An average CI of 1 indicates an additive effect, CI < 1 is synergistic and CI > 1 antagonistic. **(D)** KOPT-K1 cells were cultured for 48 h with DMSO or 3 μM of NDI-031301 in the absence or presence of SB203580 (5 or 10 μM). Cells were fixed and assessed for apoptosis by flow cytometric analysis following terminal deoxynucleotidyl transferase (TdT) dUTP nick-end labeling (TUNEL) and proppidium iodide (PI) double staining. Upper panels show two-dimensional dot plots with the percentage of TUNEL-positive cells in each treated sample. Lower panel shows quantification of TUNEL-positive cells. Values represent mean ± s.d. percentages of TUNEL-positive cells in duplicate experiments. *: $P < 0.05$ by two-sample, two-tailed *t* test. **(E)** SB203580 inhibits activation of p38 MAPK and apoptosis induced by NDI-031301. KOPT-K1 cells were cultured for 24 h with DMSO or 3 μM of NDI-031301 in the absence or presence of SB203580 (5 or 10 μM). Whole-cell extracts were analyzed by immunoblotting with each specific antibody.

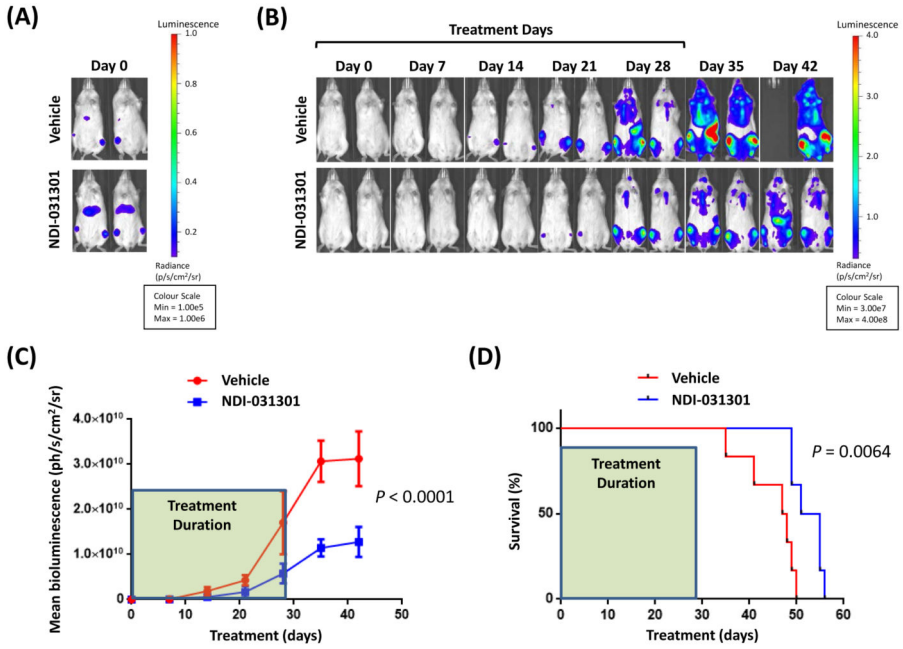

Fig 5. NDI-031301 treatment effectively suppresses the growth of KOPT-K1 cells engrafted into NSG mice and provides a significant survival benefit

(A) Bioluminescent images of two representative mice to be treated with either vehicle or NDI-031301, on day 0. Scale bar indicates the bioluminescence intensities. **(B)** Bioluminescent images of representative mice treated with either vehicle or 100 mg/kg NDI-031301 twice daily for the indicated number of days. Scale bar shows the colour variation corresponding to bioluminescence intensities. **(C)** Mean ± SEM bioluminescence of mice treated with vehicle or 100 mg/kg NDI-031301 for 29 days (n = 6 for each treatment group; statistical significance was assessed at day 42 by two-sample, two-tailed *t* test). **(D)** Kaplan-Meier survival analysis of mice treated with vehicle or 100 mg/kg NDI-031301 for 29 days (n = 6 for each treatment group; statistical significance was assessed with the log-rank test).

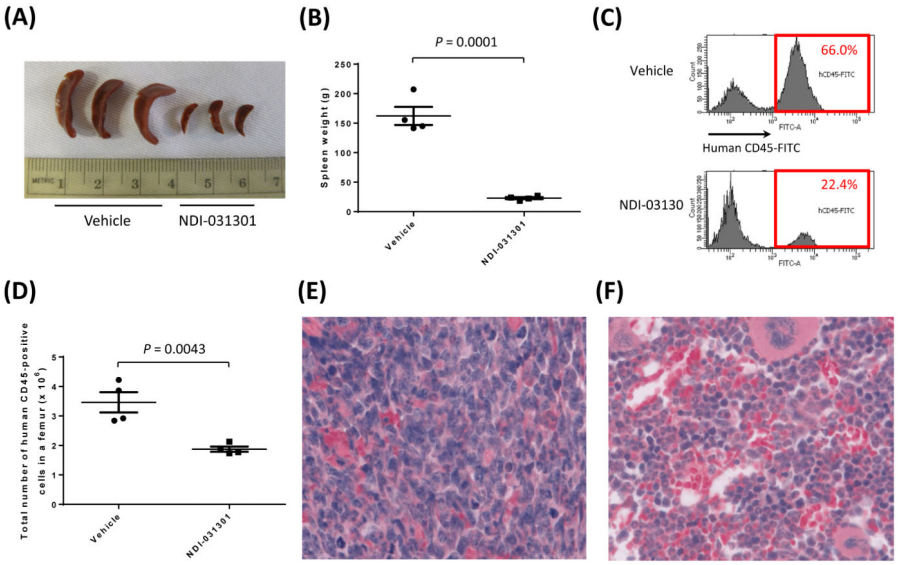

Fig 6. NDI-031301 reduces infiltration of leukaemia cells into mouse bone marrow and spleen

All samples were harvested on Day 29 after twice daily treatment with vehicle or 100 mg/kg NDI-031301 for 29 days. **(A)** A photograph of spleens from representative mice. Ruler scale is in cm. **(B)** Spleen weights. Error bars represent SEM. Statistical significance was assessed by two-sample, two-tailed *t* test. **(C)** Human CD45-FITC histogram of femur bone marrow cells in a representative mouse. The percentage of human CD45-positive cells is shown in each panel. **(D)** Total numbers of human CD45-positive cells in a femur of each treated mouse (n = 4 for each treatment group). Error bars represent SEM. Statistical significance was assessed by two-sample, two-tailed *t* test. **(E-F)** Haematoxylin and eosin staining of paraffin-embedded femur sections isolated from mice treated with vehicle **(E)** or 100 mg/kg NDI-031301 **(F)**.

Table I

Potency, JAK family selectivity, and pharmacokinetics of NDI-031301.

Potency, Selectivity and Drug-like Properties*		**NDI-031301**
Biochemical TYK2 Kinase Assay at 1 mM ATP (nM)	TYK2 Ki	130
Biochemical JAK Family Kinase Activity at 1 mM ATP (nM)	JAK1 Ki	2200
	JAK2 Ki	2750
	JAK3 Ki	2480
Cell Growth Inhibition GIC_{50} (μM)	KOPT-K1 cells	2
PPB	mouse PPB (% bound)	76
Mouse PK PO 100 mg/kg	$T_{1/2}$ (h)	4.9
	C_{max} (μM)	25

Ki, kinase inhibitor; GIC_{50}, 50% growth inhibitory concentration; PK, pharmacokinetics; PPB, plasma protein binding

*In vivo pharmacokinetic profiles of NDI-031301 in mice (C57) treated with indicated doses of inhibitor. Half-life ($T_{1/2}$) and maximum serum concentration (C_{max}) of the drug concentration-time profile are shown.